
SVMax: A Feature Embedding Regularizer

Ahmed Taha¹ Alex Hanson¹ Abhinav Shrivastava¹ Larry Davis¹

Abstract

A neural network regularizer (*e.g.*, weight decay) boosts performance by *explicitly* penalizing the complexity of a network. In this paper, we penalize inferior network activations – feature embeddings – which in turn regularize the network’s weights *implicitly*. We propose singular value maximization (SVMax) to learn a more uniform feature embedding. The SVMax regularizer supports both supervised and unsupervised learning. Our formulation mitigates model collapse and enables larger learning rates. We evaluate the SVMax regularizer using both retrieval and generative adversarial networks. We leverage a synthetic mixture of Gaussians dataset to evaluate SVMax in an unsupervised setting. For retrieval networks, SVMax achieves significant improvement margins across various ranking losses. Code available at <https://bit.ly/3jNkgDt>

1. Introduction

A neural network’s knowledge is embodied in *both* its weights and activations. This difference manifests in how network pruning and knowledge distillation tackle the model compression problem. While pruning literature (Li et al., 2016; Luo et al., 2017; Yu et al., 2018) compresses models by removing less significant weights, knowledge distillation (Hinton et al., 2015) reduces computational complexity by matching a cumbersome network’s last layer activations (logits). This perspective, of weight-knowledge versus activation-knowledge, emphasizes how neural network literature is dominated by explicit weight regularizers. In contrast, this paper leverages singular value decomposition (SVD) to regularize a network through its last layer activations – its feature embedding.

Our formulation is inspired by principal component analysis (PCA). Given a set of points and their covariance, PCA yields the set of orthogonal eigenvectors sorted by their

eigenvalues. The principal component (first eigenvector) is the axis with the highest variation (largest eigenvalue) as shown in Figure 1c. The eigenvalues from PCA, and similarly the singular values from SVD, provide insights about the feature embedding structure. As such, by regularizing the singular values, we reshape the feature embedding.

The main contribution of this paper is to leverage the singular value decomposition of a network’s activations to regularize the feature embedding. We achieve this objective through singular value maximization (SVMax). The SVMax regularizer is oblivious to both the input-class (labels) and the sampling strategy. Thus it promotes a uniform feature embedding in both supervised and unsupervised learning. Furthermore, we present a mathematical analysis of the mean singular value’s lower and upper bounds. This analysis makes tuning the SVMax’s balancing-hyperparameter easier, when the feature embedding is normalized to the unit circle.

SVMax promotes a uniform feature embedding. During training, SVMax speeds up convergence by enabling large learning rates. The SVMax regularizer integrates seamlessly with various ranking losses. We apply the SVMax regularizer to the last feature embedding layer, but the same formulation can be applied to intermediate layers. The SVMax regularizer mitigates model collapse in both retrieval networks and generative adversarial networks (GANs) (Goodfellow et al., 2014; Srivastava et al., 2017; Metz et al., 2017). Furthermore, the SVMax regularizer is useful when training self/un-supervised feature embedding networks with a contrastive loss (*e.g.*, CPC) (Noroozi et al., 2017; Oord et al., 2018; He et al., 2019; Tian et al., 2019).

In summary, we propose singular value maximization to regularize the feature embedding. In addition, we present a mathematical analysis of the mean singular value’s lower and upper bounds to reduce hyperparameter tuning (Sec. 3). We quantitatively evaluate how SVMax significantly boosts the performance of ranking losses (Sec. 4.1). And we provide a qualitative evaluation of using SVMax in the unsupervised learning setting via GAN training (Sec. 4.2).

¹University of Maryland, College Park. Correspondence to: Ahmed Taha, Alex Hanson.

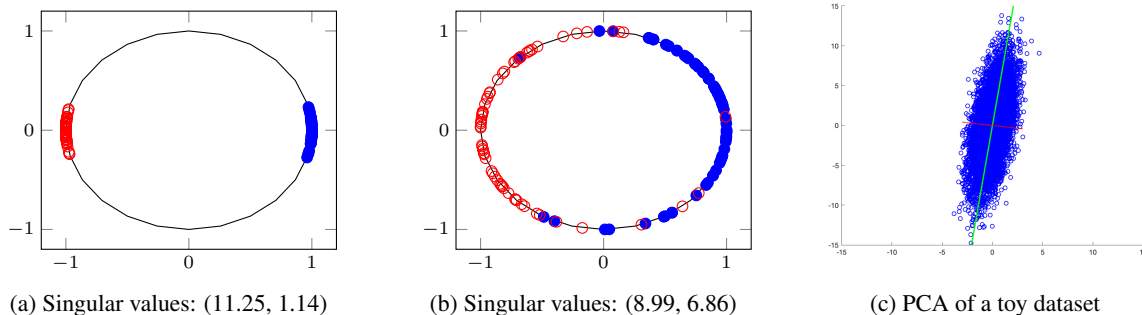


Figure 1. Feature embeddings scattered over the $2D$ unit circle. In (a), the features are polarized across a single axis; the singular value of the principal (horizontal) axis is large while the singular value of the secondary (vertical) axis is small, respectively. In (b), the features spread uniformly across both dimensions; both singular values are comparably large. (c) depicts the PCA analysis of a toy 2D Gaussian dataset to demonstrate our intuition. The principal component (green) has the highest eigenvalue, *i.e.*, the axis with the highest variation, while the second component (red) has a smaller eigenvalue. Maximizing all eigenvalues promotes data dispersion across all dimensions. In this paper, we maximize the mean singular value to regularize the feature embedding and avoid a model collapse.

2. Related Work

Network weight regularizers dominate the deep learning regularizer literature because they support a large spectrum of tasks and architectures. Singular value decomposition (SVD) has been applied as a weight regularizer in several recent works (Zhang et al., 2018; Sedghi et al., 2018; Guo & Ye, 2019). Zhang et al. (2018) employ SVD to avoid vanishing and exploding gradients in recurrent neural networks. Similarly, Guo & Ye (2019) bound the singular values of the convolutional layer around 1 to preserve the layer’s input and output norms. A bounded output norm mitigates the exploding/vanishing gradient problem. Weight regularizers share the common limitation that they do not enforce an explicit feature embedding objective and are thus ineffective against model collapse.

Feature embedding regularizers have also been extensively studied, especially for classification networks (Rippel et al., 2015; Wen et al., 2016; He et al., 2018; Hoffman et al., 2019; Taha et al., 2020). These regularizers aim to maximize class margins, class compactness, or both simultaneously. For instance, Wen et al. (2016) propose center loss to explicitly learn class representatives and thus promote class compactness. In classification tasks, test samples are assumed to lie within the same classes of the training set, *i.e.*, closed-set identification. However, retrieval tasks, such as product re-identification, assume an open-set setting. Because of this, a retrieval network regularizer should aim to spread features across many dimensions to fully utilize the expressive power of the embedding space.

Recent literature (Sablayrolles et al., 2018; Zhang et al., 2017b) has recognized the importance of a spread-out feature embedding. However, this literature is tailored to triplet loss and therefore assumes a particular sampling procedure. In this paper, we leverage SVD as a regularizer because it is simple, differentiable (Ionescu et al., 2015), and class

oblivious. SVD has been used to promote *low* rank models to learn compact intermediate layer representations (Kliegl et al., 2017; Sanyal et al., 2019). This helps compress the network and speed up matrix multiplications on embedded devices (iPhone and Raspberry Pi). In contrast, we regularize the embedding space through a *high* rank objective. By maximizing the mean singular value, we promote a higher rank representation – a spread-out embedding.

3. Singular Value Maximization (SVMax)

We first introduce our mathematical notation. Let \mathcal{I} denote the image space and $E_{\mathcal{I}} \in R^d$ denote the feature embeddings space, where d is the dimension of the features. A feature embedding network is a function $F_{\theta} : \mathcal{I} \rightarrow E_{\mathcal{I}}$, parameterized by the network’s weights θ . We quantify similarity between an image pair $(\mathcal{I}_1, \mathcal{I}_2)$ via the Euclidean distance in feature space, *i.e.*, $\|E_{\mathcal{I}_1} - E_{\mathcal{I}_2}\|_2$.

During training, a $2D$ matrix $E \in R^{b \times d}$ stores b samples’ embeddings, where b is the mini-batch size. Assuming $b \geq d$, the singular value decomposition (SVD) of E provides the singular values $S = [s_1, \dots, s_i, \dots, s_d]$, where s_1 and s_d are the largest and smallest singular values, respectively. We maximize the mean singular value, $s_{\mu} = \frac{1}{d} \sum_{i=1}^d s_i$, to regularize the network’s last layer activations – the feature embedding. By maximizing the mean singular value, the deep network spreads out its embeddings. This has the added benefit of implicitly regularizing the network’s weights θ . The proposed SVMax regularizer integrates with both supervised and unsupervised feature embedding networks as follows

$$L_{\text{NN}} = L_r - \lambda \frac{1}{d} \sum_{i=1}^d s_i = L_r - \lambda s_{\mu}, \quad (1)$$

where L_r is the original loss and λ is a hyperparameter.

Lower and Upper Bounds of the Mean Singular Value:

One caveat to equation 1 is the hyperparameter λ . It is difficult to tune since the mean singular value s_μ depends on the range of values inside E and its dimensions (b, d). Thus, changing the batch size or embedding dimension requires a different λ . To address this, we constrain the embeddings to lie on the unit circle (L2-normalized) – a common assumption in metric learning. This provides *both* lower and upper bounds on ranking losses. This will also allow us to impose lower and upper bounds on s_μ .

For an L2-normalized embedding E , the largest singular value s_1 is maximum when the matrix-rank of E equals one, *i.e.*, $rank(E) = 1$, and $s_i = 0$ for $i \in [2, d]$. Horn & Johnson (1991) provide an upper bound on this largest singular value s_1 as $s^*(E) \leq \sqrt{\|E\|_1 \|E\|_\infty}$. This holds in equality for all L2-normalized $E \in R^{b \times d}$ with $rank(E) = 1$. For an L2-normalized matrix E with $\|E\|_1 = b$, and $\|E\|_\infty = 1$, this gives:

$$s^*(E) = \sqrt{\|E\|_1 \|E\|_\infty} = \sqrt{b}. \quad (2)$$

Thus, the lower bound L on s_μ is $L = \frac{s^*(E)}{d} = \frac{\sqrt{b}}{d}$.

Similarly, an upper bound is defined on the sum of the singular values (Turkmen & Civciv, 2007; Kong et al., 2018; Friedland & Lim, 2016). This summation is formally known as the nuclear norm of a matrix $\|E\|_*$. Hu (2015) established an upper bound on this summation using the Frobenius Norm $\|E\|_F$ as follows

$$\|E\|_* \leq \sqrt{\frac{b \times d}{\max(b, d)}} \|E\|_F, \quad (3)$$

where $\|E\|_F = \left(\sum_{i=1}^{rows} \sum_{j=1}^{cols} |E_{ij}|^2 \right)^{\frac{1}{2}} = \sqrt{b}$ because of the L2-normalization assumption.

Accordingly, the lower and upper bounds of s_μ are $[L, U] = \left[\frac{s^*(E)}{d}, \frac{\|E\|_*}{d} \right]$. With these bounds, we rewrite our final loss function as follows

$$L_{NN} = L_r + \lambda \exp\left(\frac{U - s_\mu}{U - L}\right). \quad (4)$$

The SVMax regularizer grows exponentially $\in [1, e]$. We employ this loss function in all our retrieval experiments. It is important to note that the L2-normalized assumption makes λ tuning easier, but it is not required. Equation 4 makes the hyperparameter λ only dependent on the range of L_r which is also bounded for ranking losses.

Lower and Upper Bounds of Ranking Losses: We briefly show that ranking losses are bounded when assuming an L2-normalized embedding. Equations 5 and 6 show triplet and contrastive losses, respectively, and their corresponding

bounds $[L, U]$.

$$\begin{aligned} TL_{(a,p,n) \in T} &= [(D_{a,p} - D_{a,n} + m)]_+ \\ &\xrightarrow{[L,U]} [0, 2 + m], \end{aligned} \quad (5)$$

$$\begin{aligned} CL_{(x,y) \in P} &= \delta_{x,y} D_{x,y} + (1 - \delta_{x,y}) [m - D_{x,y}]_+ \\ &\xrightarrow{[L,U]} [0, 2], \end{aligned} \quad (6)$$

where $[\bullet]_+ = \max(0, \bullet)$, $m < 2$ is the margin between classes, since 2 is the maximum distance on the unit circle. $D_{x_1, x_2} = D(N(x_1), N(x_2))$; $N(\bullet)$ and $D(\bullet, \bullet)$ are the network’s output-embedding and Euclidean distance, respectively. In equation 5, a, p , and n are the anchor, positive, and negative images in a single triplet (a, p, n) from the triplets set T . In equation 6, x and y form a single pair of images from the pairs set P . $\delta_{x,y} = 1$ when x and y belong to the same class; zero otherwise. In the paper appendix, we (1) show similar analysis for N-pair and angular losses, and (2) provide an empirical SVMax evaluation on small training batches, *i.e.*, $b < d$.

4. Experiments

In this section, we evaluate SVMax using both supervised and unsupervised learning. We leverage retrieval and generative adversarial networks for quantitative and qualitative evaluations, respectively.

4.1. Retrieval Networks

Technical Details: We evaluate SVMax quantitatively using three datasets: CUB-200-2011 (Wah et al., 2011), Stanford CARS196 (Krause et al., 2013), and Stanford Online Products (Oh Song et al., 2016). We use GoogLeNet (Szegedy et al., 2015) and ResNet50 (He et al., 2016); both pretrained on ImageNet (Deng et al., 2009) and fine-tuned for K iterations. These are standard retrieval datasets and architectures. By default, the embedding $\in R^{d=128}$ is normalized to the unit circle. In all experiments, a batch size $b = 144$ is employed, the learning rate lr is fixed for $K/2$ iterations then decayed polynomially to $1e-7$ at iteration K . We use the SGD optimizer with 0.9 momentum. Each batch contains p different classes and l different samples per class. For example, triplet loss employs $p = 24$ different classes and $l = 6$ instances per class. The mini-batch of N-pair loss contains 72 classes and a single positive pair per class, *i.e.*, $p = 72$ and $l = 2$. This same mini-batch setting is used for angular loss. For contrastive loss, $p = 36$ and $l = 4$ are divided into 72 positive and 72 negative pairs. For both CUB-200 and CARS196, $K = 5,000$ iterations; for Stanford Online Products, $K = 20,000$.

Baselines: We evaluate SVMax using contrastive (Hadsell et al., 2006), hard triplet (Hoffer & Ailon, 2015; Hermans et al., 2017), N-pair (Sohn, 2016) and angular (Wang et al.,

Table 1. Quantitative evaluation on CUB-200-2011 with batch size $b = 144$, embedding dimension $d = 128$ and multiple learning rates $lr = \{0.01, 0.001, 0.0001\}$. $\Delta_{R@1}$ column indicates the R@1 improvement margin relative to the vanilla ranking loss. A large learning rate lr increases the chance of model collapse, while a small lr slows convergence. λ is dependent on the ranking loss.

Method	$lr = 0.01$				$lr = 0.001$				$lr = 0.0001$			
	NMI	R@1	R@8	$\Delta_{R@1}$	NMI	R@1	R@8	$\Delta_{R@1}$	NMI	R@1	R@8	$\Delta_{R@1}$
Contrastive												
Vanilla	0.435	25.73	58.88	-	0.443	28.68	64.70	-	0.413	24.49	59.54	-
Spread-out	0.440	24.54	57.16	-1.18	0.479	32.12	66.83	3.44	0.458	31.85	67.45	7.36
SVMMax (Ours)	0.527	41.26	75.24	15.53	0.547	43.11	77.26	14.43	0.449	29.56	65.50	5.06
Triplet Loss												
Vanilla	0.496	29.34	67.96	-	0.477	28.88	64.60	-	0.449	24.86	61.14	-
Spread-out	0.545	43.60	76.98	14.26	0.557	44.02	78.54	15.14	0.435	28.33	64.33	3.46
SVMMax $\lambda = 1$ (Ours)	0.556	43.21	77.43	13.88	0.527	39.13	74.17	10.25	0.401	25.07	60.01	0.20
SVMMax $\lambda = 0.1$ (Ours)	0.547	43.80	77.97	14.47	0.557	43.89	78.44	15.01	0.436	28.22	64.40	3.36
N-pair												
Vanilla	0.402	18.96	50.32	-	0.452	27.65	63.10	-	0.455	31.41	66.95	-
Spread-out	0.416	20.64	52.80	1.69	0.483	32.46	66.41	4.81	0.474	33.39	68.80	1.98
SVMMax (Ours)	0.483	34.62	68.11	15.67	0.547	43.79	77.31	16.14	0.488	34.13	69.92	2.72
Angular												
Vanilla	0.470	28.54	60.03	-	0.508	38.94	72.82	-	0.538	41.80	76.18	-
Spread-out	.471	28.29	60.26	-0.25	0.508	38.96	72.86	0.02	0.538	41.81	76.23	0.02
SVMMax (Ours)	0.487	32.88	66.27	4.34	0.523	41.29	74.71	2.35	0.531	42.00	76.30	0.20

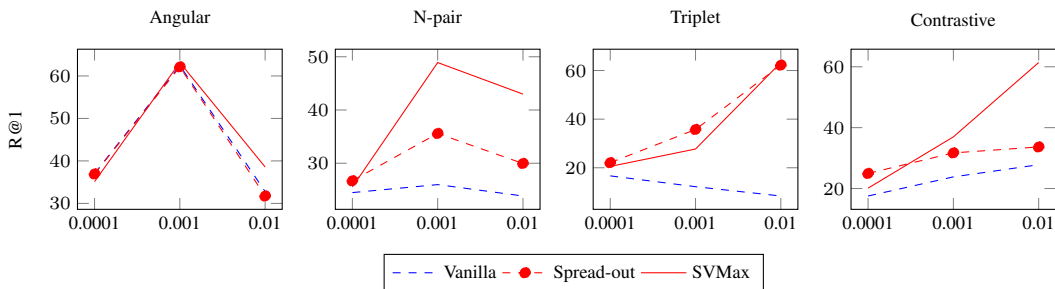


Figure 2. Quantitative evaluation on Stanford CARS196. X and Y-axis denote the learning rate lr and recall@1 performance, respectively.

2017) losses. We use the margin $m = 1$ for contrastive loss, $m = 0.2$ for triplet loss, and the angle bound $\alpha = 45^\circ$ for angular loss. Similar to SVMMax, multiple regularizers (Kumar et al., 2016; Zhang et al., 2017b; Sanyal et al., 2019; Chen & Deng, 2019) promote a uniform embedding space. Unlike SVMMax, these regularizers require a supervised setting to push anchor-negative pairs apart. We employ the spread-out regularizer (Zhang et al., 2017b) as a baseline for its simplicity, with default hyperparameter $\alpha = 1$. To enable the spread-out regularizer on non-triplet ranking losses, we pair every anchor with a random negative sample from the training mini-batch.

Evaluation Metrics: For quantitative evaluation, we use the Recall@K metric and Normalized Mutual Info (NMI) on the test split.

The hyperparameter: $\lambda = 1$ for both contrastive and N-pair losses, $\lambda = 0.1$ for triplet loss, and $\lambda = 2$ for angular loss. We fix λ across datasets, architectures, and other hyperparameters (b, d).

Results: Tables 1 and 2 present quantitative retrieval evaluation on CUB-200 and Stanford Online Products datasets – both using GoogLeNet. These tables provide in depth analysis and emphasize our improvement margins on a small and large dataset. Figure 2 provides quantitative evaluation on Stanford CARS196. We report quantitative evaluation on ResNet50 in the paper appendix. Our training hyperparameters – learning rate lr and number of iterations K – do not favor a particular ranking loss in these experiments.

We evaluate SVMMax on various learning rates. A large learning rate, e.g., $lr = 0.01$, speeds up convergence, but increases the chance of model collapse. In contrast, a small rate, e.g., $lr = 0.0001$, is likely to avoid model collapse but is slow to converge. This undesirable effect is tolerable for small datasets – where increasing the number of training iterations K does not drastically increase the overall training time – but it is infeasible for large datasets. For contrastive and N-pair losses, SVMMax significantly outperforms both the vanilla and spread-out baselines with larger learning

Table 2. Quantitative evaluation on Stanford Online Products.

Method	$lr = 0.01$				$lr = 0.001$				$lr = 0.0001$			
	NMI	R@1	R@8	$\Delta_{R@1}$	NMI	R@1	R@8	$\Delta_{R@1}$	NMI	R@1	R@8	$\Delta_{R@1}$
Contrastive												
Vanilla	0.816	18.23	34.07	-	0.820	28.70	43.27	-	0.813	34.30	48.49	-
Spread-out	0.811	18.87	35.74	0.64	0.822	29.97	46.69	1.27	0.824	36.15	51.22	1.85
SVMax (Ours)	0.875	61.82	78.90	43.59	0.854	53.94	70.92	25.25	0.832	41.96	57.44	7.66
Triplet Loss												
Vanilla	0.891	71.96	86.24	-	0.873	64.09	80.07	-	0.840	46.29	62.57	-
Spread-out	0.890	71.60	85.73	-0.36	0.872	64.23	80.10	0.14	0.840	46.68	63.04	0.39
SVMax $\lambda = 1$ (Ours)	0.868	63.82	80.95	-8.15	0.857	58.04	75.14	-6.04	0.836	44.62	60.76	-1.67
SVMax $\lambda = 0.1$ (Ours)	0.889	71.48	85.97	-0.49	0.872	64.23	80.14	0.14	0.840	46.64	62.95	0.35
N-pair												
Vanilla	0.798	12.86	24.53	-	0.815	23.83	38.97	-	0.818	33.98	48.56	-
Spread-out	0.803	16.58	31.91	3.72	0.824	32.88	50.34	9.05	0.825	37.39	52.55	3.40
SVMax (Ours)	0.871	57.76	76.05	44.90	0.858	54.70	71.57	30.87	0.835	43.04	58.78	9.06
Angular												
Vanilla	0.883	62.83	80.13	-	0.885	66.93	82.12	-	0.856	54.29	71.14	-
Spread-out	0.883	62.73	79.96	-0.10	0.885	66.91	82.09	-0.02	0.856	54.30	71.10	0.02
SVMax (Ours)	0.885	65.44	81.73	2.61	0.884	67.28	82.47	0.35	0.855	54.88	71.47	0.59

rates. A small lr slows convergence and all approaches are roughly equivalent. The spread-out regularizer (Zhang et al., 2017b) and its hyperparameters are tuned for triplet loss. Thus, for this particular ranking loss, the SVMax and spread-out regularizers are on par.

In our experiments, we employ a large learning rate because it is the simplest factor to induce model collapse. However, the learning rate is not the only factor. Another factor is the training dataset size and its intra-class variations. A small dataset with large intra-class variations increases the chances of a model collapse. For example, a pair of dissimilar birds from the same class justifies a model collapse when coupled with a large learning rate. The hard triplet loss experiments emphasize this point because every anchor is paired with the hardest positive and negative samples. On small fine-grained datasets like CUB-200 or CARS196, the vanilla hard triplet loss suffers significantly. Yet, the same implementation is superior on a big dataset like Stanford Online Products. By carefully tuning the training hyperparameter on CUB-200, it is possible to avoid a degenerate solution. However, this tedious tuning process is unnecessary when using either the spread-out or the SVMax regularizer.

The vanilla N-pair loss underperforms because it does not support feature embedding on the unit circle. Both spread-out and SVMax mitigate this limitation. For angular loss, a bigger $\lambda = 2$ is employed to cope with the angular loss range. SVMax is a class oblivious regularizer. Thus, λ should be significant enough to contribute to the loss function without dominating the ranking loss.

Wu et al. (2017) show that the distance between any anchor-negative pair, which is randomly sampled from an n -dimensional unit sphere, follows the normal distribution

$N(\sqrt{2}, \frac{1}{2n})$. This mean distance $\sqrt{2}$ is large relative to the triplet loss margin $m = 0.2$, but comparable to the contrastive loss margin $m = 1$. Accordingly, triplet loss converges to zero after a few iterations, because most triplets satisfy the margin $m = 0.2$ constraint. When triplet loss equals zero, the SVMax regularizer with $\lambda = 1$ becomes the dominant term. However, SVMax should not dominate because it is oblivious to data annotations; it equally pushes anchor-positive and anchor-negative pairs apart. Reducing λ to 0.1 solves this problem.

A less aggressive triplet loss (Schroff et al., 2015; Xuan et al., 2020) is another way to avoid model collapse. For instance, Schroff et al. (2015) have proposed a triplet loss variant that employs semi-hard negatives. The semi-hard triplet loss is more stable than the aggressive hard triplet and lifted structured losses (Oh Song et al., 2016). Unfortunately, the semi-hard triplet loss assumes a large mini-batch ($b = 1,800$ in Schroff et al. (2015)), which is impractical. Furthermore, when model collapse is avoided, aggressive triplet loss variants achieve superior performance (Hermans et al., 2017). In contrast, SVMax only requires a larger mini-batch than the embedding dimension, *i.e.*, $b \geq d$, a natural constraint for retrieval networks which favor compact embedding dimensions. Additionally, SVMax makes no assumptions about the sampling procedure. Thus, unlike (Sablayrolles et al., 2018; Zhang et al., 2017b), SVMax supports various supervised ranking losses.

SVMax and SOTA results: In the previous experiments (tables 1 and 2), we did not tune our hyperparameters to a particular ranking loss. The best hyperparameters for angular loss achieve inferior performance on contrastive loss and vice versa. Thus, we choose learning rates uniformly [0.01, 0.001, 0.0001]. In order to achieve SOTA results, it is im-

Table 3. Quantitative retrieval evaluation using Proxy-Anchor loss on three datasets: CUB-200, Stanford Cars, and Stanford Online Products (SOP). The performance is reported on both Inception-BN and ResNet50 architectures using Recall@1.

	CUB	CARS	SOP
Inception-BN			
Vanilla	66.92±0.002	84.67±0.002	79.02±0.001
SVMMax $\lambda = 10^{-3}$ (Ours)	67.00±0.008	84.73±0.002	79.04±0.000
SVMMax $\lambda = 10^{-4}$ (Ours)	67.16±0.003	84.74±0.002	79.04±0.001
ResNet50			
Vanilla	68.37±0.003	87.30±0.001	80.06±0.007
SVMMax $\lambda = 10^{-3}$ (Ours)	68.67±0.004	87.39±0.002	79.26±0.007
SVMMax $\lambda = 10^{-4}$ (Ours)	68.45±0.005	87.64±0.003	79.52±0.004

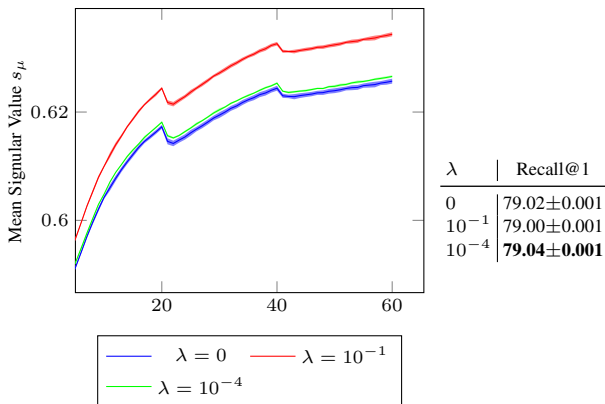


Figure 3. Stanford Online Products experiment. **Left:** Quantitative evaluation of s_μ while training for 60 epochs. **Right:** Quantitative retrieval evaluation using recall@1 metric.

portant to tune hyperparameters (lr , # iterations), leverage a large embedding dimension ($d = 512$), and freeze certain layers (e.g., batch norm). In the following experiment, we evaluate SVMMax on the Proxy-Anchor loss (Kim et al., 2020).

Table 3 presents a quantitative retrieval evaluation using Proxy-Anchor. For these experiments, we set the embedding dimension $d = 512$. We use a mini-batch $b = 512$ with Inception-BN (Ioffe & Szegedy, 2015) and $b = 256$ with ResNet50 (He et al., 2016). To achieve SOTA results on different datasets and architectures, Proxy-Anchor tunes *five* hyperparameters¹: number of warm-up epochs, learning rate, whether to freeze batch norm or not, learning rate decay step, and learning rate decay gamma. This intense hyperparameter tuning explains why SVMMax has marginal effect on Proxy-Anchor. We recommend a single $\lambda = 10^{-4}$ across all architectures and datasets. We report performance using both $\lambda = \{10^{-3}, 10^{-4}\}$ to highlight SVMMax’s stability.

The bounds of the mean singular value s_μ enable us to evaluate the feature embedding quantitatively. In the Inception-

¹<https://github.com/tjddus9597/Proxy-Anchor-CVPR2020>

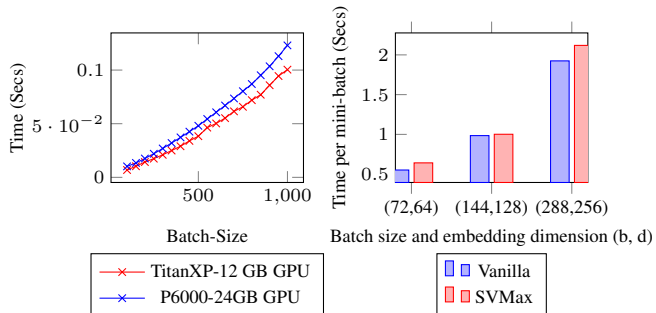


Figure 4. (Left) Timing analysis for the Tensorflow (TF) `tf.linalg.svd` function. The x-axis denotes the batch size b , and the y-axis denotes the running time in seconds. We time this TF function using two different GPUs. (Right) Timing analysis for a mini-batch training time using MobileNet. The x-axis denotes both the batch size b and the embedding dimension d . The y-axis denotes the batch training time in seconds.

BN experiment ($b = d = 512$), the upper and lower bounds of s_μ are $[L, U] = [0.044, 1]$. Figure 3 depicts s_μ during training on Stanford Online Products for 60 epochs, and the learning rate decays every 20 epochs. The figure depicts s_μ using three different λ values. We repeat each experiment five times and report the mean s_μ (solid line) and standard deviation (filled-area). The vanilla Proxy-Anchor loss maximizes s_μ without SVMMax ($\lambda = 0$). With $\lambda = 10^{-1}$, SVMMax regularizes the feature embedding and maximizes s_μ , but recall@1 (R@1) decreases by 0.02%. SVMMax with $\lambda = 10^{-4}$ maximizes s_μ while boosting R@1.

Weight decay imposes a prior on the network weights. Similarly, SVMMax imposes a prior on the network activations. Both priors are important but they should never dominate the loss function. Thus, a large λ (e.g., 1 or 0.1) is undesirable if the hyperparameters are already tuned to achieve state-of-the-art results.

SVMMax’s Computational Complexity: We compute the singular values $S = [s_1, \dots, s_i, \dots, s_d]$ using TensorFlow (TF) `tf.linalg.svd`. This function runs on the GPU. We did not notice any computational overhead or numerical instability during training. Figure 4 (Left) provides a timing analysis of the TF function using square matrices. For a typical mini-batch size ($b < 256$), the function takes around 0.01 seconds. This speed depends on the GPU specification and recent GPUs would perform faster. Figure 4 (Right) provides a timing analysis for the mini-batch training time using MobileNet. SVMMax adds minimal overhead compared to the overhead of performing gradient descent on a deep network. We conclude that for a reasonable batch size b and embedding dimension d , SVMMax adds minimal computational complexity to the training process.

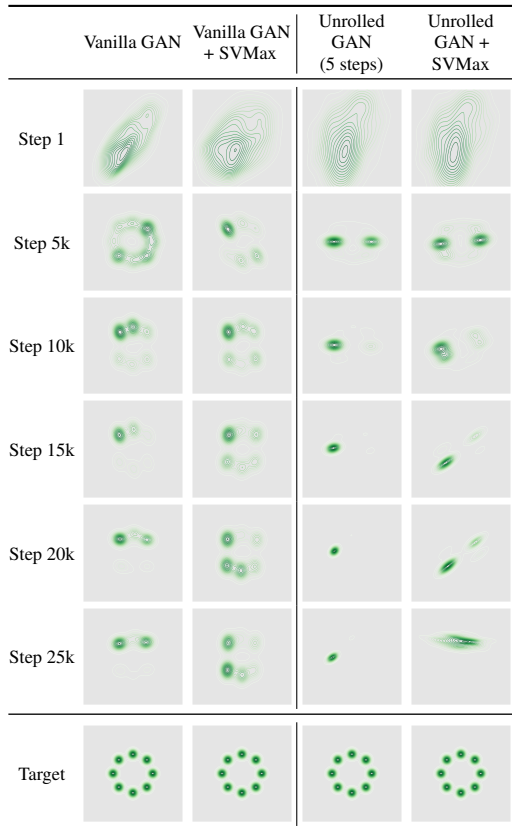


Figure 5. SVMMax mitigates model collapse in a GAN trained on a toy 2D mixture of Gaussians dataset. Rows show heatmaps of the generator distributions at different training steps. The final row shows the groundtruth distribution. The first column shows the distributions generated by training a vanilla GAN suffering a model collapse. The second column shows the generated distribution when penalizing the generator’s fake embedding with SVMMax. The third and fourth columns show two distributions generated using an unrolled-GAN without and with SVMMax, respectively. This high resolution figure is best viewed on a screen with zoom capabilities.

4.2. Generative Adversarial Networks

Model collapse is one of the main challenges of training generative adversarial networks (GANs) (Metz et al., 2017; Srivastava et al., 2017; Mao et al., 2019; Salimans et al., 2016). To tackle this challenge, Metz et al. (2017) propose an unrolled-GAN to prevent the generator from overfitting to the discriminator. In an unrolled-GAN, the generator observes the discriminator for l steps before updating the generator’s parameters using the gradient from the final step. Alternatively, we leverage the simpler SVMMax regularizer to avoid model collapse. We evaluate our regularizer using a simple GAN on a 2D mixture of 8 Gaussians arranged in a circle. This 2D baseline (Metz et al., 2017; Srivastava et al., 2017; Bang & Shim, 2018) provides a simple qualitative evaluation and demonstrates SVMMax’s potential in unsuper-

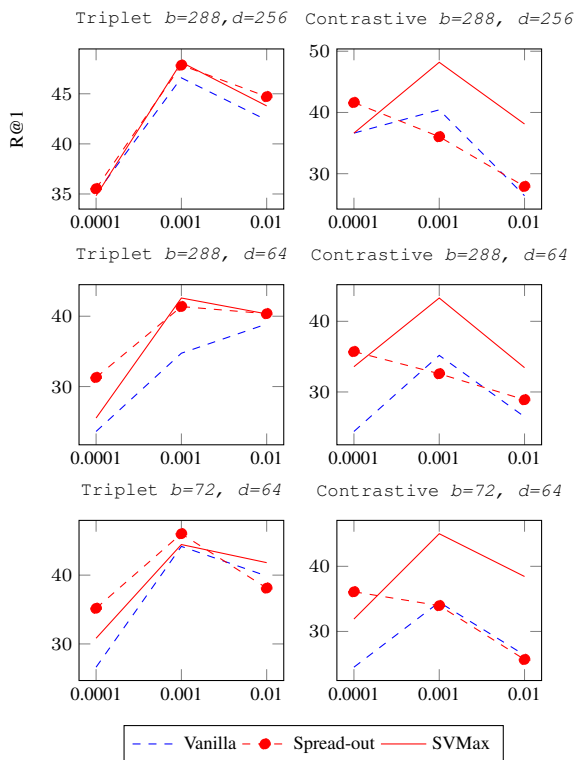


Figure 6. Quantitative evaluation on CUB-200-2011 with various batch sizes $b = \{288, 72\}$ and embedding dimensions $d = \{256, 64\}$ to demonstrate the stability of our hyperparameter. $\lambda = 1$ for contrastive loss and $\lambda = 0.1$ for triplet loss.

vised learning. We leverage this simple baseline because we assume $b \geq d$, which does not hold for images.

Figure 5 shows the dynamics of the GAN generator through time. We use a public PyTorch implementation² of (Metz et al., 2017). We made a single modification to the code to use a relatively large learning rate, *i.e.*, $lr = 0.025$ for both the generator and discriminator. This single modification is a simple and fast way to induce model collapse. The mixture of Gaussians circle has a radius $r = 2$, *i.e.*, the generated fake embedding is neither L2-normalized nor strictly bounded by a network layer. We kept the radius parameter unchanged to emphasize that neither L2-normalization nor strict-bounds are required. To mitigate the impact of lurking variables (*e.g.*, random network initialization and mini-batch sampling), we fix the random generator’s seed for all experiments. We apply SVMMax to a vanilla and an unrolled GAN for five steps. We apply the unbounded SVMMax regularizer (Eq. 1), *i.e.*, $L_{NN} = L_{GAN} - \lambda s_{\mu}$, where $\lambda = 0.01$ and s_{μ} is mean singular value of the generator fake embedding.

GANs are typically used to generate high resolution images. This high-resolution output is the main limitation of

²<https://github.com/andrewliao11/unrolled-gans>

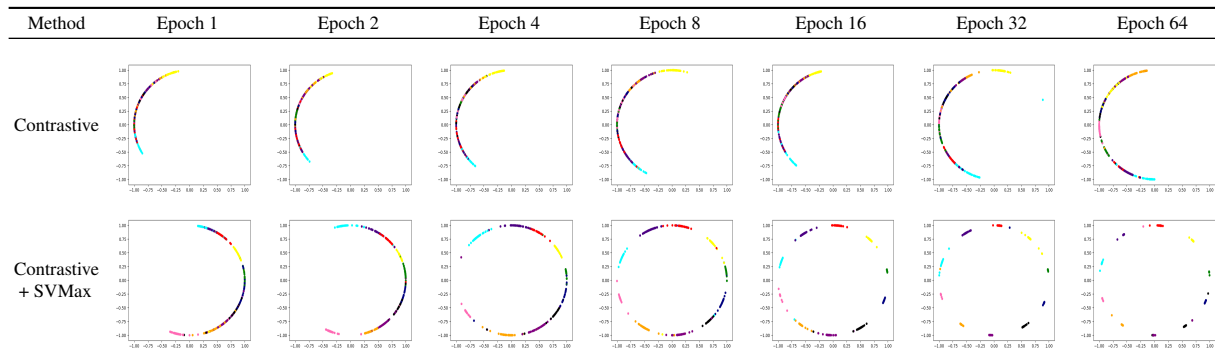


Figure 7. Qualitative feature embedding evaluation using the MNIST dataset projected onto the 2D unit circle. The first row shows the feature embedding learned using a vanilla contrastive loss and the second row applies the SVMMax regularizer. A random subset of the test split is projected for visualization purpose. Different colors denote different classes. The regularized feature embedding spreads out uniformly and rapidly. The supplementary material shows the feature embedding evolves vividly up to 200 epochs. This high resolution figure is best seen on a screen.

the SVMMax regularizer. The *current* formulation assumes the batch size is bigger than the embedding dimension, *i.e.*, $b \geq d$. This constraint is trivial for the Gaussians mixture 2D dataset and retrieval networks with a compact embedding dimensionality (*e.g.*, $d = \{128, 256\}$). However, this constraint hinders high resolution image generators because the mini-batch size constraint becomes $b \geq W \times H \times C$, where W , H , and C are the generated image’s width, height, and number of channels, respectively. Nevertheless, this GAN experiment emphasizes the potential of the SVMMax regularizer in unsupervised learning.

If the batch-size limitation is set aside, the following points are worth noting: (I) Image-synthesis GANs have bounded outputs $[0, 255]$; White images will not fool the discriminator. Thus, s_μ remains bounded but with different bounds from those presented in the approach section. (II) Alain & Bengio (2016) (§3.4) address practical concerns when working with high dimensional features. (III) GANs have synthesized not only high quality images, but also feature embeddings (Zhu et al., 2018).

4.3. Ablation Study

In this section, we evaluate two hypotheses: (1) the same SVMMax hyperparameter λ supports different embedding dimensions and batch sizes – the main objective of the mean singular value’s bounds analysis, (2) the SVMMax regularizer boosts retrieval performance because it learns a uniform feature embedding.

The mean singular value bound analysis makes tuning the hyperparameter λ easier. This hyperparameter becomes only dependent on the ranking loss’s range and independent of both the batch size and the embedding dimension. Figure 6 presents a quantitative evaluation using the CUB-200 dataset. We explore various batch sizes $b = \{288, 72\}$ and

embedding dimensions $d = \{256, 64\}$. We employ a MobileNetV2 (Sandler et al., 2018) to fit the big batch $b = 288$ on a 24GB GPU. The paper appendix contains a similar evaluation on the Stanford Online Products and CARS196 datasets.

To evaluate SVMMax’s impact on feature embeddings, we embed the MNIST dataset onto the 2D unit circle. In this experiment, we use a tiny CNN (one convolutional layer and one hidden layer). Figure 7 shows the feature embedding after training for t epochs. With SVMMax, the feature embeddings spread out more uniformly and rapidly than the vanilla contrastive loss.

5. Conclusion

We have proposed singular value maximization (SVMMax) as a feature embedding regularizer. SVMMax promotes a uniform embedding, mitigates model collapse, and enables large learning rates. Unlike other embedding regularizers, SVMMax supports a large spectrum of ranking losses. Moreover, it is oblivious to data annotation and, as such, supports both supervised and unsupervised learning. Qualitative evaluation using a generative adversarial network demonstrates SVMMax’s potential in unsupervised learning. Quantitative retrieval evaluation highlight significant performance improvements due to the SVMMax regularizer.

Acknowledgments: This work was partially funded by independent grants from Office of Naval Research (N000141612713) and Facebook AI. AH was supported by the NDSEG fellowship.

References

Alain, G. and Bengio, Y. Understanding intermediate layers using linear classifier probes. *arXiv preprint*

- arXiv:1610.01644*, 2016.
- Bang, D. and Shim, H. Mgan: Solving mode collapse using manifold guided training. *arXiv preprint arXiv:1804.04391*, 2018.
- Caron, M., Misra, I., Mairal, J., Goyal, P., Bojanowski, P., and Joulin, A. Unsupervised learning of visual features by contrasting cluster assignments. *arXiv preprint arXiv:2006.09882*, 2020.
- Chen, B. and Deng, W. Energy confused adversarial metric learning for zero-shot image retrieval and clustering. In *AAAI*, 2019.
- Chen, T., Kornblith, S., Norouzi, M., and Hinton, G. A simple framework for contrastive learning of visual representations. In *ICML*, 2020.
- Chen, X. and He, K. Exploring simple siamese representation learning. *arXiv preprint arXiv:2011.10566*, 2020.
- Deng, J., Dong, W., Socher, R., Li, L.-J., Li, K., and Fei-Fei, L. Imagenet: A large-scale hierarchical image database. In *CVPR*, 2009.
- Doersch, C., Gupta, A., and Efros, A. A. Unsupervised visual representation learning by context prediction. In *ICCV*, 2015.
- Donahue, J., Krähenbühl, P., and Darrell, T. Adversarial feature learning. *arXiv preprint arXiv:1605.09782*, 2016.
- Friedland, S. and Lim, L.-H. The computational complexity of duality. *SIAM Journal on Optimization*, 26(4):2378–2393, 2016.
- Goodfellow, I., Pouget-Abadie, J., Mirza, M., Xu, B., Warde-Farley, D., Ozair, S., Courville, A., and Bengio, Y. Generative adversarial nets. In *NIPS*, 2014.
- Grill, J.-B., Strub, F., Altché, F., Tallec, C., Richemond, P. H., Buchatskaya, E., Doersch, C., Pires, B. A., Guo, Z. D., Azar, M. G., et al. Bootstrap your own latent: A new approach to self-supervised learning. *arXiv preprint arXiv:2006.07733*, 2020.
- Guo, P. and Ye, Q. On regularization for a convolutional kernel in neural networks. *arXiv preprint arXiv:1906.04866*, 2019.
- Hadsell, R., Chopra, S., and LeCun, Y. Dimensionality reduction by learning an invariant mapping. In *CVPR*, 2006.
- He, K., Zhang, X., Ren, S., and Sun, J. Deep residual learning for image recognition. In *CVPR*, 2016.
- He, K., Fan, H., Wu, Y., Xie, S., and Girshick, R. Momentum contrast for unsupervised visual representation learning. *arXiv preprint arXiv:1911.05722*, 2019.
- He, X., Zhou, Y., Zhou, Z., Bai, S., and Bai, X. Triplet-center loss for multi-view 3d object retrieval. *arXiv preprint arXiv:1803.06189*, 2018.
- Hermans, A., Beyer, L., and Leibe, B. In defense of the triplet loss for person re-identification. *arXiv preprint arXiv:1703.07737*, 2017.
- Hinton, G., Vinyals, O., and Dean, J. Distilling the knowledge in a neural network. *arXiv preprint arXiv:1503.02531*, 2015.
- Hoffer, E. and Ailon, N. Deep metric learning using triplet network. In *International Workshop on Similarity-Based Pattern Recognition*, 2015.
- Hoffman, J., Roberts, D. A., and Yaida, S. Robust learning with jacobian regularization. *arXiv preprint arXiv:1908.02729*, 2019.
- Horn, R. A. and Johnson, C. R. Topics in matrix analysis cambridge university press. *Cambridge, UK*, 1991.
- Hu, S. Relations of the nuclear norm of a tensor and its matrix flattenings. *Linear Algebra and its Applications*, 478:188–199, 2015.
- Ioffe, S. and Szegedy, C. Batch normalization: Accelerating deep network training by reducing internal covariate shift. *arXiv preprint arXiv:1502.03167*, 2015.
- Ionescu, C., Vantzos, O., and Sminchisescu, C. Training deep networks with structured layers by matrix backpropagation. *arXiv preprint arXiv:1509.07838*, 2015.
- Kim, S., Kim, D., Cho, M., and Kwak, S. Proxy anchor loss for deep metric learning. In *CVPR*, 2020.
- Kliegl, M., Goyal, S., Zhao, K., Srinet, K., and Shoeybi, M. Trace norm regularization and faster inference for embedded speech recognition rnns. *arXiv preprint arXiv:1710.09026*, 2017.
- Kong, X., Li, J., and Wang, X. New estimations on the upper bounds for the nuclear norm of a tensor. *Journal of inequalities and applications*, 2018(1):282, 2018.
- Krause, J., Stark, M., Deng, J., and Fei-Fei, L. 3d object representations for fine-grained categorization. In *Proceedings of the IEEE international conference on computer vision workshops*, 2013.
- Kumar, B., Carneiro, G., Reid, I., et al. Learning local image descriptors with deep siamese and triplet convolutional networks by minimising global loss functions. In

- Proceedings of the IEEE Conference on Computer Vision and Pattern Recognition*, pp. 5385–5394, 2016.
- Li, H., Kadav, A., Durdanovic, I., Samet, H., and Graf, H. P. Pruning filters for efficient convnets. *arXiv preprint arXiv:1608.08710*, 2016.
- Luo, J.-H., Wu, J., and Lin, W. Thinet: A filter level pruning method for deep neural network compression. In *ICCV*, 2017.
- Mao, Q., Lee, H.-Y., Tseng, H.-Y., Ma, S., and Yang, M.-H. Mode seeking generative adversarial networks for diverse image synthesis. In *CVPR*, 2019.
- Metz, L., Poole, B., Pfau, D., and Sohl-Dickstein, J. Unrolled generative adversarial networks. In *ICLR*, 2017.
- Noroozi, M. and Favaro, P. Unsupervised learning of visual representations by solving jigsaw puzzles. In *ECCV*, 2016.
- Noroozi, M., Pirsivash, H., and Favaro, P. Representation learning by learning to count. In *ICCV*, 2017.
- Oh Song, H., Xiang, Y., Jegelka, S., and Savarese, S. Deep metric learning via lifted structured feature embedding. In *CVPR*, 2016.
- Oord, A. v. d., Li, Y., and Vinyals, O. Representation learning with contrastive predictive coding. *arXiv preprint arXiv:1807.03748*, 2018.
- Pathak, D., Krahenbuhl, P., Donahue, J., Darrell, T., and Efros, A. A. Context encoders: Feature learning by inpainting. In *CVPR*, 2016.
- Rippel, O., Paluri, M., Dollar, P., and Bourdev, L. Metric learning with adaptive density discrimination. *arXiv preprint arXiv:1511.05939*, 2015.
- Sablayrolles, A., Douze, M., Schmid, C., and Jégou, H. Spreading vectors for similarity search. *arXiv preprint arXiv:1806.03198*, 2018.
- Salimans, T., Goodfellow, I., Zaremba, W., Cheung, V., Radford, A., and Chen, X. Improved techniques for training gans. In *NIPS*, 2016.
- Sandler, M., Howard, A., Zhu, M., Zhmoginov, A., and Chen, L.-C. Mobilenetv2: Inverted residuals and linear bottlenecks. In *CVPR*, 2018.
- Sanyal, A., Kanade, V., and Torr, P. H. S. Learning low-rank representations. *arXiv preprint arXiv:1804.07090*, 2019.
- Schroff, F., Kalenichenko, D., and Philbin, J. Facenet: A unified embedding for face recognition and clustering. In *CVPR*, 2015.
- Sedghi, H., Gupta, V., and Long, P. M. The singular values of convolutional layers. *arXiv preprint arXiv:1805.10408*, 2018.
- Sohn, K. Improved deep metric learning with multi-class n-pair loss objective. In *NIPS*, 2016.
- Srivastava, A., Valkov, L., Russell, C., Gutmann, M. U., and Sutton, C. Veegan: Reducing mode collapse in gans using implicit variational learning. In *NSIP*, 2017.
- Szegedy, C., Liu, W., Jia, Y., Sermanet, P., Reed, S., Anguelov, D., Erhan, D., Vanhoucke, V., and Rabinovich, A. Going deeper with convolutions. In *CVPR*, 2015.
- Taha, A., Chen, Y.-T., Misu, T., Shrivastava, A., and Davis, L. Boosting standard classification architectures through a ranking regularizer. In *WACV*, 2020.
- Tian, Y., Krishnan, D., and Isola, P. Contrastive multiview coding. *arXiv preprint arXiv:1906.05849*, 2019.
- Turkmen, R. and Civeci, H. Some bounds for the singular values of matrices. *Applied Mathematical Sciences*, 1 (49):2443–2449, 2007.
- Wah, C., Branson, S., Welinder, P., Perona, P., and Belongie, S. The caltech-ucsd birds-200-2011 dataset. 2011.
- Wang, J., Zhou, F., Wen, S., Liu, X., and Lin, Y. Deep metric learning with angular loss. In *ICCV*, 2017.
- Wen, Y., Zhang, K., Li, Z., and Qiao, Y. A discriminative feature learning approach for deep face recognition. In *ECCV*, 2016.
- Wu, C.-Y., Manmatha, R., Smola, A. J., and Krahenbuhl, P. Sampling matters in deep embedding learning. In *ICCV*, 2017.
- Xuan, H., Stylianou, A., and Pless, R. Improved embeddings with easy positive triplet mining. In *WACV*, 2020.
- Yu, R., Li, A., Chen, C.-F., Lai, J.-H., Morariu, V. I., Han, X., Gao, M., Lin, C.-Y., and Davis, L. S. Nisp: Pruning networks using neuron importance score propagation. In *CVPR*, 2018.
- Zhang, J., Lei, Q., and Dhillon, I. S. Stabilizing gradients for deep neural networks via efficient svd parameterization. *arXiv preprint arXiv:1803.09327*, 2018.
- Zhang, R., Isola, P., and Efros, A. A. Colorful image colorization. In *ECCV*, 2016.
- Zhang, R., Isola, P., and Efros, A. A. Split-brain autoencoders: Unsupervised learning by cross-channel prediction. In *CVPR*, 2017a.

Zhang, X., Yu, F. X., Kumar, S., and Chang, S.-F. Learning spread-out local feature descriptors. In *ICCV*, 2017b.

Zhu, Y., Elhoseiny, M., Liu, B., Peng, X., and Elgammal, A. A generative adversarial approach for zero-shot learning from noisy texts. In *CVPR*, 2018.

The following appendix sections A and B extend their corresponding sections in the main paper. For instance, the extended-approach appendix A extends the approach section in the main paper.

A. Appendix: Extended Approach

This section presents the lower and upper bounds of N-pair and angular losses and analyzes a *theoretical* corner case for SVMax.

A.1. N-pair and Angular Losses

Lower and Upper Bounds of Ranking Losses: The N-pair and angular losses are bounded when their feature embeddings are L2-normalized. These bounds depend on the number of negative samples inside the training mini-batch B . Each mini-batch contains a single positive pair of samples per class, $\{a, p\}$, with all remaining samples, n , representing negative samples of that class. a, p, n denote the anchor, positive and negative samples, respectively. This gives $|n| = b - 2$ as the number of negative samples w.r.t. a mini-batch of size b . Both losses also use the inner product operation to quantify similarity between feature embeddings, *i.e.*, $\in [-1, 1]$, allowing us to find our bounds. Equation 7 shows the N-pair loss (NL) formulation:

$$\text{NL} = -\log \frac{\exp(\lfloor a \rfloor \lfloor p \rfloor)}{\exp(\lfloor a \rfloor \lfloor p \rfloor) + \sum_{n \in B} \exp(\lfloor a \rfloor \lfloor n \rfloor)}, \quad (7)$$

where each n is a negative sample, a is the anchor, and p is the positive sample inside the mini-batch B . $\lfloor \bullet \rfloor$ is the embedding function (encoder). Thus, the lower and upper bounds for the L2-normalized N-pair loss are the following:

$$[L, U]_{\text{NL}} = [\log(e^2 + |n|) - 2, \log(e^2|n| + 1)]. \quad (8)$$

Equations 9 and 10 show the angular loss (AL) formulation:

$$\text{AL} = \log \left[1 + \sum_{n \in B} \exp(f_{a,p,n}) \right], \quad (9)$$

$$\begin{aligned} \text{s.t. } f_{a,p,n} &= 4 \tan^2 \alpha (\lfloor a \rfloor + \lfloor p \rfloor)^T \lfloor n \rfloor \\ &\quad - 2(1 + \tan^2 \alpha) \lfloor a \rfloor^T \lfloor p \rfloor, \end{aligned} \quad (10)$$

where, again, each n is a negative sample, a is the anchor, p is the positive sample inside the mini-batch B , and $\lfloor \bullet \rfloor$ is the embedding function (encoder). The parameter α is a hyperparameter chosen before training and is thus a fixed value. As such, the lower and upper bounds for L2-normalized $f_{a,p,n}$ are:

$$[L, U]_{f_{a,p,n}} = [-10 \tan^2 \alpha - 2, 6 \tan^2 \alpha - 2]. \quad (11)$$

We use $\alpha = 45^\circ$ in all our experiments. This gives $\tan \alpha = 1$, $[L, U]_{f_{a,p,n}} \in [-12, 4]$ and our angular loss bounds as:

$$[L, U]_{\text{AL}} = [\log(e^{-12}|n| + 1), \log(e^4|n| + 1)]. \quad (12)$$

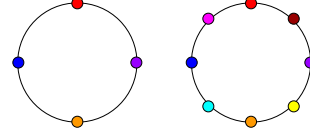


Figure 8. The feature embeddings of two independent mini-batches with $p = 4$ (Left) and $p = 8$ (Right) classes on the 2D unit circle. Different colors denote different classes. The mean singular value s_μ is maximum if (1) samples from the same class have zero standard deviation and (2) the p sampled classes are distributed perfectly in the embedding space.

A.2. SVMax Corner Case

Theoretically, the mean singular value s_μ can reach its upper bound for a mini-batch, even if the feature embedding is not perfectly uniform. During training, each mini-batch contains p different classes and l different samples per class, *i.e.*, the batch size $b = p \times l$. The sampled classes p in a mini-batch is smaller than the number of total classes C in the dataset, *i.e.*, $p < C$. If (1) the sampled p classes are perfectly distributed in the feature embedding and (2) the l samples for each class have zero standard deviation, the mean singular value equals the upper bound ($s_\mu = U$) even if the feature embedding for the whole dataset is not uniform. Figure 8 illustrates this scenario.

In practice, this will never happen during training because (1) the feature embedding dimension is large enough (*e.g.*, $d = 128$), (2) samples in the training mini-batches are randomly sampled, and (3) samples are independent across mini-batches. This corner case is omitted from the main paper because it undermines the paper’s flow and clarity.

B. Appendix: Extended Experiments

Section B.1 provides further quantitative evaluations for SVMax when $b \geq d$. Then, Section B.2 evaluates SVMax with small mini-batches, *i.e.*, $b < d$. Finally, Section B.3 evaluates SVMax using self-supervised learning. The supplementary *video* vividly shows how SVMax speeds convergence on the MNIST dataset.

B.1. Retrieval Networks

Evaluation Metrics: For quantitative evaluation, we leverage the **Recall@K** metric and **Normalized Mutual Info** (NMI) on the test split. The NMI score evaluates the quality of cluster alignments. $\text{NMI} = \frac{I(\Omega, C)}{\sqrt{H(\Omega)H(C)}}$, where $\Omega = \{\omega_1, \dots, \omega_n\}$, is the ground-truth clustering, while $C = \{c_1, \dots, c_n\}$ is a clustering assignment for the learned embedding. $I(\bullet, \bullet)$ and $H(\bullet)$ denote mutual information and entropy, respectively. We use K-means to compute C .

Quantitative Evaluation: In the main paper, SVMax is

Table 4. Quantitative evaluation using N-pair loss without L2-normalization on three datasets and GoogLeNet with batch size $b = 144$, embedding dimension $d = 128$ and multiple learning rates $lr = \{0.01, 0.001, 0.0001\}$. $\Delta_{R@1}$ column indicates the R@1 improvement margin relative to the vanilla ranking loss. SVMax leverages the upper and lower bounds while SVMax'' does not.

Method	$lr = 0.01$				$lr = 0.001$				$lr = 0.0001$			
	NMI	R@1	R@8	$\Delta_{R@1}$	NMI	R@1	R@8	$\Delta_{R@1}$	NMI	R@1	R@8	$\Delta_{R@1}$
N-pair on CUB-200-2011												
Vanilla	0.560	46.08	79.09	-	0.553	44.24	78.12	-	0.555	45.32	78.71	-
Spread-out	degenerate (Trm loss \rightarrow nan)			-	0.560	45.80	78.66	1.55	0.537	42.67	77.16	-2.65
SVMax'' (Ours)	0.563	45.80	79.73	-0.29	0.553	44.90	78.58	0.66	0.555	44.97	78.80	-0.35
SVMax (Ours)	0.561	46.27	79.86	0.19	0.563	46.40	79.69	2.16	0.563	45.70	79.27	0.37
N-pair on Stanford CARS196												
Vanilla	0.606	65.49	90.32	-	0.5983	64.92	90.00	-	0.480	44.13	79.77	-
Spread-out	degenerate (Trm loss \rightarrow nan)			-	0.109	2.58	14.07	-62.34	0.393	31.53	67.85	-12.59
SVMax'' (Ours)	0.606	65.45	90.87	-0.04	0.592	64.92	90.08	0.00	0.481	44.25	79.93	0.12
SVMax (Ours)	0.611	69.72	92.15	4.23	0.601	67.31	91.33	2.39	0.492	48.73	83.18	4.60
N-pair on Stanford Online Products												
Vanilla	0.897	74.54	87.92	-	0.884	69.34	84.46	-	0.863	59.68	76.42	-
Spread-out	degenerate (Trm loss \rightarrow nan)			-	0.877	64.23	80.34	-5.11	0.858	56.50	73.15	-3.18
SVMax'' (Ours)	0.897	74.82	88.30	0.28	0.883	69.30	84.49	-0.05	0.864	59.69	76.43	0.01
SVMax (Ours)	0.895	74.44	87.91	-0.10	0.882	69.52	84.62	0.17	0.864	59.93	76.73	0.26

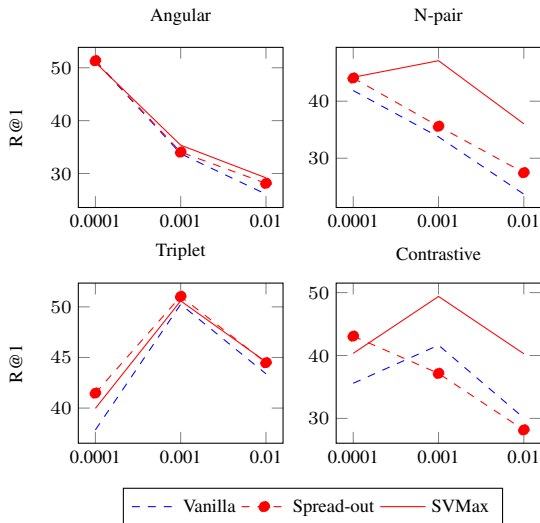


Figure 9. Quantitative evaluation on CUB-200-2011 using ResNet50. The X axis denotes the learning rate lr and the Y-axis denotes recall@1 performance.

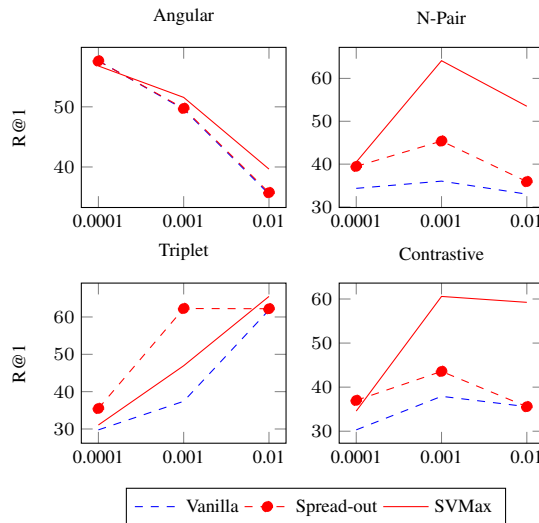


Figure 10. Quantitative evaluation on Stanford CARS196 using ResNet50.

evaluated quantitatively using GoogLeNet. Figures 9 and 10 present quantitative evaluation using ResNet50 on CUB-200-2011 and Stanford CARS196, respectively.

Our evaluation hyperparameters (*e.g.*, learning rate and batch size) do not favor a particular ranking loss. The ideal hyperparameters depend on the ranking loss and other factors such as the dataset size, batch size, and network architecture. The hyperparameters in the main paper are inconsistent with the N-pair loss because this loss assumes an un-normalized embedding. Table 4 presents an SVMax evaluation using un-normalized embedding on three datasets.

We leverage both the unbound SVMax (SVMax'') in equation 13 and the bounded SVMax (SVMax) in equation 14. Surprisingly, the bounded SVMax, which assumes an L2-normalized embedding, achieves competitive performance on the un-normalized embedding. It is important to note that while N-pair loss assumes an un-normalized embedding, N-pair loss *regularizes* the L2-norm of the embedding vectors to be small. Table 4 shows that the spread-out regularizer degenerates severely, while SVMax remains resilient. The spread-out regularizer requires an L2-normalized embedding while SVMax does not. In Table 4, the unbound SVMax uses $\lambda = 0.01$ while the bounded SVMax uses $\lambda = 1$.

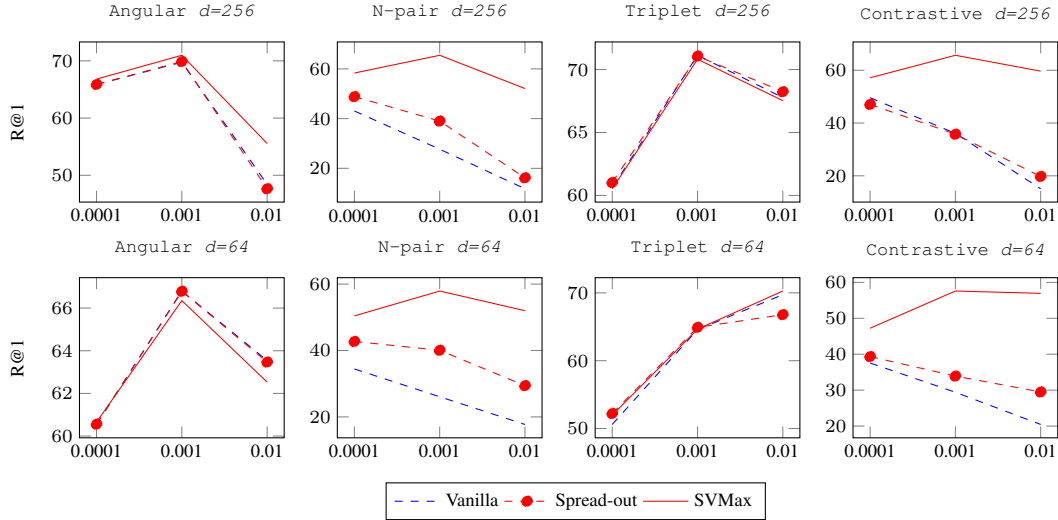


Figure 11. Quantitative evaluation on Stanford Online Products using various embedding dimensions $d = \{256, 64\}$ to demonstrate the stability of our hyperparameter.

$$L_{\text{NN}} = L_r - \lambda \frac{1}{d} \sum_{i=1}^d s_i = L_r - \lambda s_\mu, \quad (13)$$

$$L_{\text{NN}} = L_r + \lambda \exp\left(\frac{U - s_\mu}{U - L}\right). \quad (14)$$

Figures 11 and 12 present a quantitative evaluation with various embedding dimensions. We use batch sizes $b = \{288, 72\}$ and embedding dimensions $d = \{256, 64\}$. In this experiment, we employ a MobileNetV2 (Sandler et al., 2018) to fit our neural network on a 24GB GPU. The N-pair and angular loss evaluations are dropped in Figure 12 because these losses assume a single pair of anchor-positive per class. The CARS196, with 98 training classes, is too small to provide $144 = \frac{288}{2}$ anchor-positive pairs.

In the main paper, we discuss two factors that contribute to model collapse in retrieval networks: learning rate and dataset intra-class variations. However, additional factors can also contribute. For instance, the likelihood of model collapse decreases as the mini-batch size b increases. In the early training stages, a large learning rate will induce a noisy gradient. A large training mini-batch mitigates this noisy gradient and learns a better feature embedding. The next section evaluates SVMMax with small training mini-batches.

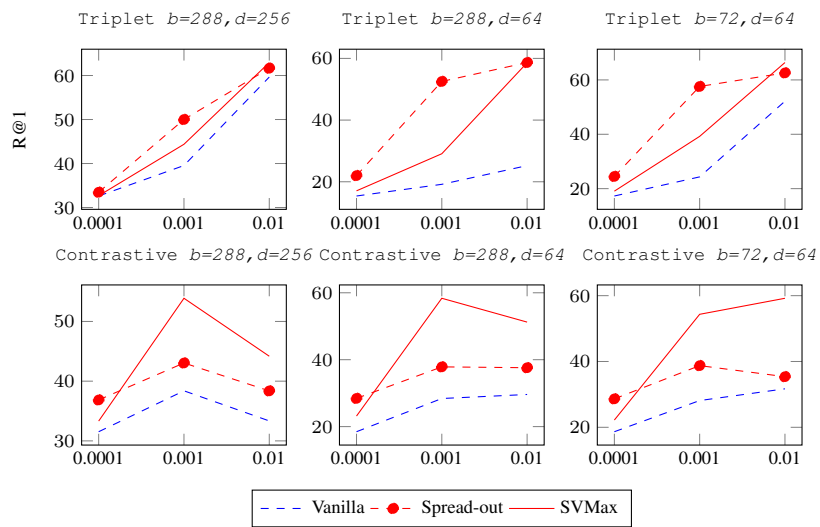


Figure 12. Quantitative evaluation on Stanford CARS196 using MobileNet, various embedding dimensions $d = \{256, 64\}$, and batch sizes $b = \{288, 72\}$ to demonstrate the stability of our hyperparameter. $\lambda = 1$ and 0.1 for contrastive and triplet loss, respectively.

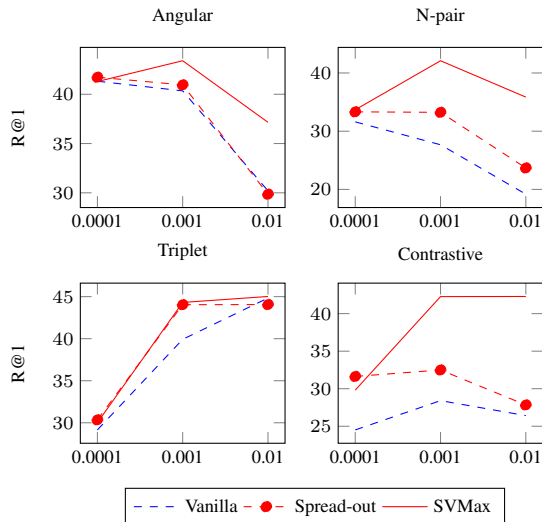


Figure 13. Quantitative evaluation on CUB-200-2011 using GoogLeNet with $b = 72$ and $d = 128$, *i.e.*, $b < d$.

B.2. SVMax with Small Batches

In the approach section, we assumed $b \geq d$ to deliver a rigorous mathematical foundation for SVMax. In this section, we present empirical evidence to support SVMax with small mini-batches. When $b < d$, there will be at most b singular values, instead of d . The lower and upper bounds of SVMax, per mini-batch, become $[L, U] = [\frac{\sqrt{b}}{b}, \sqrt{\frac{b \times d}{\max(b, d)} \frac{\sqrt{b}}{b}}]$. It is possible that SVMax will utilize only b dimensions of the feature embedding space. We argue against this possibility using a toy example. Consider the following two mini-batches $(m_1, m_2) \in \mathbb{R}^{3 \times d}$

$$m_1 = \begin{bmatrix} m_{11} \\ m_{12} \\ m_{13} \end{bmatrix} = \begin{bmatrix} 1 & 0 & 0 & 0 & \dots & 0 \\ 0 & 1 & 0 & 0 & \dots & 0 \\ 0 & 0 & 1 & 0 & \dots & 0 \end{bmatrix}, \quad (15)$$

$$m_2 = \begin{bmatrix} m_{21} \\ m_{22} \\ m_{23} \end{bmatrix} = \begin{bmatrix} 1 & 0 & 0 & 0 & \dots & 0 \\ 0 & 1 & 0 & 0 & \dots & 0 \\ 0 & 0 & 1 & 0 & \dots & 0 \end{bmatrix}, \quad (16)$$

where the mini-batch size $b = 3$. Each individual mini-batch utilizes only the first three dimensions, *i.e.*, $\text{rank}(m_1) = \text{rank}(m_2) = 3$. While all other dimensions $[4, d]$ contain zeros, the maximum mean singular value is feasible with only the first three dimensions. However, due to the random sampling procedure, a future mini-batch m_3 will contain elements from both m_1 and m_2 . For instance, $m_3 = [m_{11} \ m_{21} \ m_{22}]^T$ will have a $\text{rank}(m_3) = 2$. For the mini-batch m_3 , the mean singular value is not maximum. To maximize s_μ , one feasible solution is to keep utilizing only the first three dimensions. However, this solution is like tossing a coin N times and expecting N heads. It is a feasible solution but unlikely.

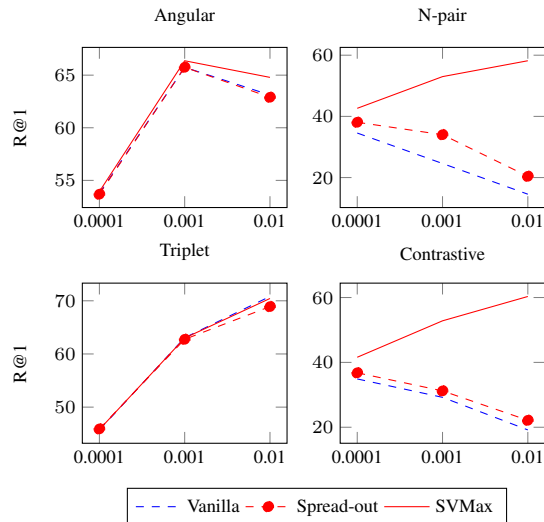


Figure 14. Quantitative evaluation on Stanford Online Products using GoogLeNet with $b = 72$ and $d = 128$, *i.e.*, $b < d$.

Figure 13 presents a quantitative evaluation using CUB-200 on GoogLeNet with $b = 72$ and $d = 128$. Similarly, Figure 14 presents a quantitative evaluation using Stanford Online Products. SVMax consistently outperforms the vanilla and spread-out baselines even when $b < d$.

Finally, Figure 15 depicts the mean singular value on the test split of CUB-200. We train our network using (1) contrastive loss with and without SVMax, and (2) different mini-batch sizes $b = \{72, 144\}$. We fix the embedding dimension $d = 128$ to study the batch size’s impact, *i.e.*, $b < d$ versus $b \geq d$. The test split of CUB-200 has 5924 test images. Thus, the upper bound of the mean singular value $U = \sqrt{\frac{b \times d}{\max(b, d)} \frac{\sqrt{b}}{d}} = 6.80$, where $b = 5924$ and $d = 128$ for the *whole* test split. After training our network, the actual mean singular value $s_\mu = 5.64$ with batch size $b = 72$, and $s_\mu = 5.81$ with $b = 144$. These mean singular values significantly outperform their vanilla contrastive loss counterparts ($s_\mu = 1.9$). Compared to $b = 144$, s_μ is smaller when using the mini-batch size $b = 72$. At a mini-batch level, SVMax spreads the feature embedding across $d = 128$ dimensions when $b = 144$, while SVMax spreads the feature embedding across $d = 72$ dimensions when $b = 72$. Yet, the comparable s_μ (5.64 versus 5.81) indicates that SVMax supports $b < d$.

B.3. Self-Supervised Learning

Another form of model collapse is a loss function with a trivial solution. This form manifests in the two terms of

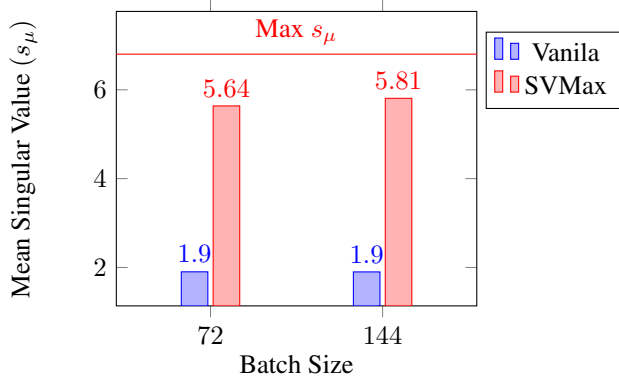


Figure 15. The mean singular values s_μ for networks trained with an embedding dimension $d = 128$. The X and Y-axes denote the mini-batch size b and the s_μ of the feature embedding of CUB-200’s test split. The feature embedding is learned using a contrastive loss with and without SVMMax. The horizontal red line denotes the upper bound on s_μ . With SVMMax, s_μ decreases marginally with $b = 72$ compared to $b = 144$. Thus, the SVMMax still promotes a uniform feature embedding even when $b < d$.

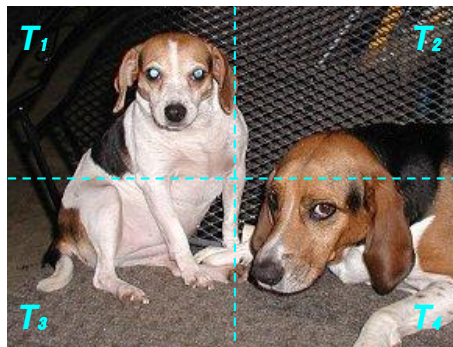
contrastive loss Eq. 17 as follows

$$\text{CL}_{(x,y) \in P} = \delta_{x,y} D_{x,y} + (1 - \delta_{x,y}) [m - D_{x,y}]_+, \quad (17)$$

where $D_{x_1, x_2} = D(N(x_1), N(x_2))$; $N(\bullet)$ and $D(\bullet, \bullet)$ are the network’s output-embedding and Euclidean distance, respectively. While the first term pulls similar points together, the second term pushes different points apart. Without the second term, contrastive loss suffers a model collapse, *i.e.*, the trivial solution $N(x) = 0, \forall x$. In supervised metric learning, similar and different classes are labeled. Thus, it is trivial to leverage contrastive loss with both terms. However, it is non-trivial to leverage contrastive loss in un/self-supervised learning.

To avoid this trivial solution, different methods have been proposed for un/self-supervised learning. For example, SimCLR (Chen et al., 2020) repels random images – assuming they belong to different classes. Other approaches like SwAV (Caron et al., 2020) leverages online clustering, while BYOL (Grill et al., 2020) leverages a momentum encoder. Recently, SimSiam (Chen & He, 2020) utilize a stop-gradient operation to avoid model collapse. All these methods deliver SOTA results, but they make assumptions about the problem formulation. For example, both SimCLR and SwAV require a large batch (e.g., 4096) to work well. In the following experiment, we show that SVMMax avoids model collapse without making assumptions about the problem formulation.

To evaluate SVMMax in self-supervised learning, we first introduce representation counting (Rep-Cnt) (Noroozi et al., 2017). Rep-Cnt is a simple self-supervised approach that counts visual primitives. Given an input image I , Rep-



Tile	Nose	Eye	Ear	Paws
T_1	1	2	2	0
T_2	0	0	0	0
T_3	0	0	0	3
T_4	1	2	2	1
I (Total)	2	4	4	4

Figure 16. An image I is split into four tiles T_i , where $i \in \{1, 2, 3, 4\}$. To learn an image representation, Rep-Cnt trains a network N such that counts of visual primitives in I equals the total visual primitives in T_i as shown in the table – $N(I) = \sum_{i=1}^4 N(T_i)$.

Cnt splits I into four tiles T_i , where $i \in \{1, 2, 3, 4\}$ as shown in Fig. 16. Rep-Cnt trains a neural network N to count visual primitives in I and T_i . The network is trained to maintain the equivariance relation. The equivariance relation requires that the count of visual primitives in I equals the total visual primitives from the four tiles, *i.e.*, $N(I) = \sum_{i=1}^4 N(T_i)$. Unfortunately, this simple self-supervised signal has a trivial solution, *i.e.*, $N(x) = 0, \forall x$. To avoid the trivial solution, Rep-Cnt is formulated as follows

$$L = \mathbb{D}_{I, T_i} + \underbrace{[m - \mathbb{D}_{I, T_i}]_+}_{\text{Problem-specific}} \quad (18)$$

where $\mathbb{D}_{I, T_i} = D(N(I), \sum_{i=1}^4 N(T_i))$. The second term pushes the representation of a random image \hat{I} from $(\sum_{i=1}^4 N(T_i))$, *i.e.*, the representation of I . This loss formulation explains how a problem-specific loss term is always required to avoid model collapse. Similarly, a different self-supervised pretext requires a different problem-specific formulation. Instead, we propose SVMMax, a generic prior, to promote a uniform feature embedding.

To integrate SVMMax in Rep-Cnt, we replace the problem-specific term with our generic prior as follows

$$L = \mathbb{D}_{I, T_i} - \lambda \underbrace{s_\mu}_{\text{Generic-prior}} \quad (19)$$

where s_μ is the mean singular value of the mini-batch embeddings $N(I)$. We leverage the unbounded SV-

Table 5. Quantitative SVMMax evaluation using self-supervised learning. We evaluate the pretrained network N through ImageNet classification with a linear classifier on top of frozen convolutional layers. For every layer, the convolutional features are spatially resized until there are fewer than 10K dimensions left. A fully connected layer followed by softmax is trained on a 1000-way object classification task. * denotes our implementation of the baseline.

Method	conv1	conv2	conv3	conv4	conv5
Supervised	19.3	36.3	44.2	48.3	50.5
Random	11.6	17.1	16.9	16.3	14.1
Context (Doersch et al., 2015)	16.2	23.3	30.2	31.7	29.6
Jigsaw (Noroozi & Favaro, 2016)	18.2	28.8	34.0	33.9	27.1
ContextEncoder (Pathak et al., 2016)	14.1	20.7	21.0	19.8	15.5
Adversarial (Donahue et al., 2016)	17.7	24.5	31.0	29.9	28.0
Colorization (Zhang et al., 2016)	12.5	24.5	30.4	31.5	30.3
Split-Brain (Zhang et al., 2017a)	17.7	29.3	35.4	35.2	32.8
Rep-Cnt* (Noroozi et al., 2017)	18.9	30.7	33.9	30.6	26.0
Rep-Cnt+SVMMax'' (Eq. 19 $\lambda = 10$)	19.4	29.3	31.7	28.9	24.5
Rep-Cnt+SVMMax'' (Eq. 19 $\lambda = 100$)	19.2	29.4	31.8	29.3	25.3

Max formulation ($-\lambda s_\mu$) instead of the bounded SVMMax ($\lambda \exp\left(\frac{U-s_\mu}{U-L}\right)$) because vector-norms satisfy the triangle inequality property, *i.e.*, $\|x+y\|^2 \leq \|x\|^2 + \|y\|^2$. If we normalize the output embedding, the $N(I) = \sum_{i=1}^4 N(T_i)$ objective becomes infeasible.

To evaluate SVMMax quantitatively, we follow Rep-Cnt technical details. We use AlexNet with three fully connected layers. The last fully connected layer provides a feature embedding. Thus, we reduce the layer’s dimension from 1000 to 128. This reduces the computational cost of SVMMax. We set $m = 10$ in Eq. 18 as in (Noroozi et al., 2017). We pretrain the AlexNet network using both Eq. 18 and Eq. 19 as a self-supervision signal. For each pretrained network, we train a linear classifier on top of the frozen CNN layers using ImageNet (Deng et al., 2009). This evaluation configuration is proposed by (Zhang et al., 2016).

Table 5 presents a quantitative SVMMax evaluation in self-supervised learning. We applied SVMMax on Rep-Cnt because it is a simple baseline. Rep-Cnt + SVMMax does not achieve state-of-the-art results. However, SVMMax can be applied on top of various self-supervised pretexts. Through this experiment, we demonstrate how SVMMax avoids a model collapse in self-supervised learning. SVMMax avoids the trivial solution without the need for a problem-specific repulsion term, an input-reconstruction term, or an adversarial loss term.